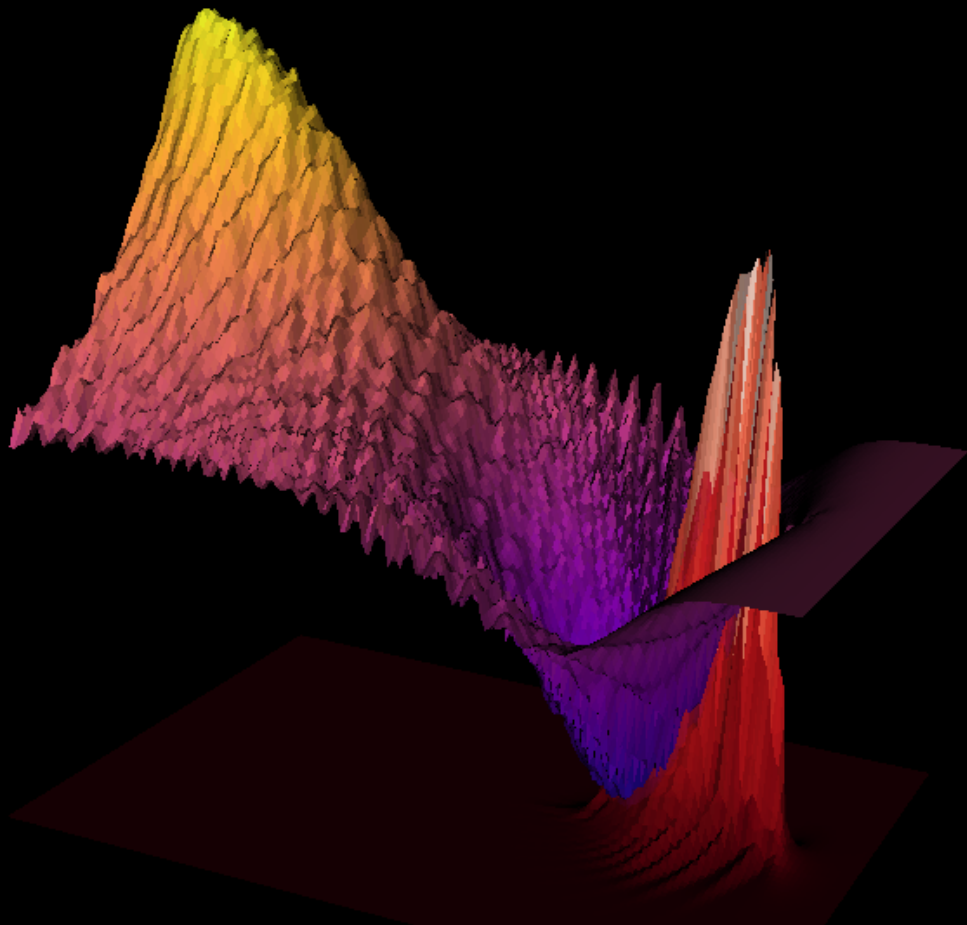


MASTER'S THESIS 2019

A compact plasma beam dump for next generation particle accelerators

OSCAR JAKOBSSON

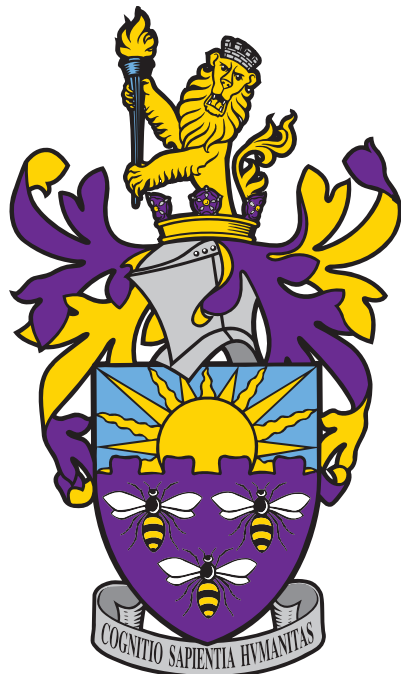


SCHOOL OF PHYSICS AND ASTRONOMY
THE UNIVERSITY OF MANCHESTER



A compact plasma beam dump for next generation particle accelerators

OSCAR JAKOBSSON



School of Physics and Astronomy
Cockcroft Accelerator Group
THE UNIVERSITY OF MANCHESTER
Manchester, United Kingdom 2019

A compact plasma beam dump for next generation particle accelerators
OSCAR JAKOBSSON

© OSCAR JAKOBSSON, 2017.

Supervisor: Guoxing Xia, Cockcroft Accelerator Group

Master's Thesis 2019
School of Physics and Astronomy
Cockcroft Accelerator Group
The University of Manchester

Cover: Wind visualization constructed in Matlab showing a surface of constant wind speed along with streamlines of the flow.

Typeset in L^AT_EX

A compact plasma beam dump for next generation particle accelerators

OSCAR JAKOBSSON

School of Physics and Astronomy

The University of Manchester

Abstract

Lore ipsum dolor sit amet, consectetur adipisicing elit, sed do eiusmod tempor incididunt ut labore et dolore magna aliqua. Ut enim ad minim veniam, quis nostrud exercitation ullamco laboris nisi ut aliquip ex ea commodo consequat. Duis aute irure dolor in reprehenderit in voluptate velit esse cillum dolore eu fugiat nulla pariatur. Excepteur sint occaecat cupidatat non proident, sunt in culpa qui officia deserunt mollit anim id est laborum.

Keywords: Plasma wakefield acceleration, deceleration, beam dump, ILC, EuPRAXIA

Acknowledgements

 Lorem ipsum dolor sit amet, consectetur adipisicing elit, sed do eiusmod tempor incididunt ut labore et dolore magna aliqua. Ut enim ad minim veniam, quis nostrud exercitation ullamco laboris nisi ut aliquip ex ea commodo consequat. Duis aute irure dolor in reprehenderit in voluptate velit esse cillum dolore eu fugiat nulla pariatur. Excepteur sint occaecat cupidatat non proident, sunt in culpa qui officia deserunt mollit anim id est laborum.

Oscar Jakobsson, Manchester, January 2019

Contents

1	Introduction	1
1.1	Conventional accelerators	1
1.2	Plasma wakefield accelerators	1
1.3	EuPRAXIA	1
1.4	Thesis Outline	1
2	Theory	3
2.1	PWFA - Linear-Fluid Wakefield Theory	3
2.1.1	Plasma Dynamics - fluid model	3
2.1.2	Density perturbations	3
2.1.3	Longitudinal Accelerating Field	4
2.1.4	Transverse Focusing Field	7
2.2	Non-linear Regime	8
2.2.1	Wave-breaking field	8
2.3	Particle interactions with matter	11
2.3.1	Bohr-Fermi-Bethe-Bloch Theory	11
2.3.2	Collective Plasma Deceleration – Non-Linear regime	11
2.3.3	Collective Plasma Deceleration – Linear regime	11
2.3.4	Notes Bonatto	12
3	Simulations	13
3.1	Particle-in-Cell Simulations	13
3.1.1	EPOCH	13
3.1.2	Grid settings	14
3.2	Notes.	16
4	Preliminary Results	17
4.1	Plasma deceleration - Uniform and varying density	17
4.2	Hybrid Scheme - Feasibility study	17
4.2.1	Initialising a decelerated bunch	17
4.2.2	Introduction of co-propagating laser	17
5	Conclusion	19
Bibliography		21
A	Appendix: Input decks	I

Contents

1

Introduction

1.1 Conventional accelerators

Conventional accelerators, RF cavities and limited acceleration , beam dump for small to future accelerators, difficulties of beam dumping only getting worse with increasing energy.

1.2 Plasma wakefield accelerators

Plasma wakefield accelerators as an alternative to accelerators. History (Tajima/Dawson), how it works, progress/challenges. Recent research also shows that L/PWFA may be a good substitute for the deceleration of the beam as well, regardless of whether the beam is accelerated in wake fields or RF cavities. Describe previous work Tajima's paper (passive), Hanahoe (varying density), Bonatto (active). In this thesis we explore these schemes, and attempt to merge the active and varying density approach in what we call a hybrid scheme. All simulations are carried out with a 1GeV 30pc so-called EuPRAXIA electron beam.

1.3 EuPRAXIA

EuPRAXIA (European Plasma Research Accelerator with eXcellence In Applications)

1.4 Thesis Outline

This intermediate report details the initial phase of a full-year project on plasma wakefield deceleration and is written in partial fulfilment of the requirements for the degree of Master in Physics. As such, it does not attempt to cover the full scope of the work and research conducted in the first half of this project, but rather aims to provide and introduction to the field, establish the theoretical background and construct the computational framework necessary to perform the research we desire. Having lain the groundwork for the project in this report, the the final-year report will reap the rewards of this work by presenting the full results and outcome of the project.

Sections:

- Theory (PWFA, LWFA, energy loss etc.)
- Simulation (PIC, EPOCH description, set up framework (“building the experiment”))
- Preliminary results (low res results) (wide bunch, varying plasma density, hybrid scheme)(Nothing

1. Introduction

conclusive just results to show that the simulations have been set up correctly)

- Conclusion + looking ahead

2

Theory

2.1 PWFA - Linear-Fluid Wakefield Theory

2.1.1 Plasma Dynamics - fluid model

What is the wave-breaking field E_Z , why is it the maximum possible acceleration/deceleration field? Is it always reached?

$$\omega_p = \sqrt{\frac{4\pi e^2 n_0}{m_e}} \quad (2.1)$$

2.1.2 Density perturbations

Continuity equation

$$\frac{\partial n}{\partial t} = -\nabla \cdot (n\mathbf{v}) \quad (2.2)$$

where n is the plasma density and \mathbf{v} the plasma fluid velocity. Charge conservation.
Lorentz force law:

$$m_e \frac{\partial n\mathbf{v}}{\partial t} = en \left(\mathbf{E} + \frac{\mathbf{v} \times \mathbf{B}}{c} \right) \quad (2.3)$$

Treating the plasma response to a particle beam perturbatively we have $n(r, z, t) = n_0 + n_1(r, z, t)$ where n_0 is the ion density and n_1 the plasma perturbation. We let $\mathbf{v}, \mathbf{E}, \mathbf{B}$ be perturbative responses to the beam. From continuity equation we have

$$\frac{\partial n_0}{\partial t} + \frac{\partial n_1}{\partial t} = -\nabla \cdot (n_0\mathbf{v}) - \nabla \cdot (n_1\mathbf{v}) \quad \Rightarrow \quad \frac{\partial n_1}{\partial t} \approx -n_0 \nabla \cdot (\mathbf{v}) \quad (2.4)$$

From the Lorentz force law have

$$m_e n_0 \frac{\partial(1 + n_1/n_0)\mathbf{v}}{\partial t} \approx en_0(1 + n_1/n_0)\mathbf{E} \quad \Rightarrow \quad m_e \frac{\partial \mathbf{v}}{\partial t} \approx e\mathbf{E} \quad (2.5)$$

which, using Gauss's law, gives

$$\frac{\partial(\nabla \cdot \mathbf{v})}{\partial t} \approx \frac{e}{m_e} \nabla \cdot \mathbf{E} = \frac{e^2}{m_e} 4\pi(n_1 + n_b) \quad (2.6)$$

where $n_1 + n_b$ is the free charge. Hence

$$\frac{\partial^2 n_1}{\partial t^2} = -n_0 \frac{\partial(\nabla \cdot \mathbf{v})}{\partial t} = -\frac{4\pi n_0 e^2}{m_e} (n_1 + n_b) \quad (2.7)$$

which gives

$$\frac{\partial^2 n_1}{\partial t^2} + \omega_p^2 n_1 = -\omega_p^2 n_b \quad (2.8)$$

where the $\omega_p = (4\pi e^2 n_0 / m_e)^{1/2}$ is the plasma frequency. We can rewrite this expression in the reference frame of the beam.

Perturbation due to beam $n(r, \xi) \rightarrow n(r, \xi) + n_1(r, \xi)$, use Maxwell's equations and continuity equation.

$$-\frac{1}{k_p^2} \left(\frac{\partial^2}{\partial \xi^2} + k_p^2 \right) n_1(r, \xi) = n_b(r, \xi) , \quad n_1(r, \xi < 0) = 0 \quad (2.9)$$

$$\mathcal{L}_\xi n_1(r, \xi) = n_b(r, \xi) \Rightarrow \mathcal{L}_\xi G(\xi, \xi') = \delta(\xi - \xi') \quad (2.10)$$

$$G(\xi, \xi') = \begin{cases} 0 & , -\infty < \xi < \xi' \\ A \sin(k_p \xi) + B \cos(k_p \xi) & , \xi' < \xi < \infty \end{cases} \quad (2.11)$$

where the Green's function obeys the same b.c as the density perturbation, i.e it is continuous across the boundary with a discontinuous derivative across the boundary. Integrate across discontinuity at $\xi = 0$

$$\lim_{\epsilon \rightarrow 0} \int_{\xi' - \epsilon}^{\xi' + \epsilon} \mathcal{L}_\xi G(\xi, \xi') d\xi = \lim_{\epsilon \rightarrow 0} \int_{\xi' - \epsilon}^{\xi' + \epsilon} \delta(\xi) d\xi = 1 \Rightarrow \lim_{\epsilon \rightarrow 0} \left[-\frac{1}{k_p^2} \frac{\partial G}{\partial \xi} \right]_{\xi' - \epsilon}^{\xi' + \epsilon} = 1 \quad (2.12)$$

Without loss of generality we may set the arrival of the beam to be at $t = 0$, such that $\xi' = 0$.

$$G(\xi, \xi') = -k_p \sin(k_p \xi) \Theta(\xi) \Rightarrow n_1(r, \xi) = \int_{-\infty}^{\infty} G(\xi, \xi') n_b(r, \xi') d\xi' \quad (2.13)$$

2.1.3 Longitudinal Accelerating Field

$$\nabla \times \mathbf{E} = -\frac{1}{c} \frac{\partial \mathbf{B}}{\partial t} \quad (2.14)$$

$$\nabla \times \mathbf{B} = \frac{4\pi}{c} \mathbf{J} + \frac{1}{c} \frac{\partial \mathbf{B}}{\partial t} \quad (2.15)$$

gives

$$\nabla^2 \mathbf{E} - \frac{1}{c^2} \frac{\partial^2 \mathbf{E}}{\partial t^2} = \frac{4\pi}{c^2} \frac{\partial \mathbf{J}}{\partial t} + 4\pi \nabla \rho \quad (2.16)$$

Lorentz force law (\mathbf{v} is the velocity of the plasma):

$$m \frac{\partial n \mathbf{v}}{\partial t} = en \left(\mathbf{E} + \frac{\mathbf{v} \times \mathbf{B}}{c} \right) \approx en \mathbf{E} \Rightarrow \frac{\partial \mathbf{J}_p}{\partial t} = \frac{e^2 n}{m} \mathbf{E} \quad (2.17)$$

Letting $\rho = \rho_b + \rho_p$ and $\mathbf{J} = \mathbf{J}_b + \mathbf{J}_p$ for the beam and plasma respectively, and $\mathbf{J}_b = c \rho_b \hat{\mathbf{z}}$, gives

$$\left(\nabla^2 - \frac{1}{c^2} \frac{\partial^2}{\partial t^2} - k_p^2 \right) \mathbf{E} = \frac{4\pi}{c} \frac{\partial \rho_b}{\partial t} \hat{\mathbf{z}} + 4\pi \nabla (\rho_b + \rho_p) \quad (2.18)$$

where $k_p = \omega_p/c$ is the plasma wave number. To find the electric field along the beam, z-direction, we proceed by solving

$$\left(\nabla^2 - \frac{1}{c^2} \frac{\partial^2}{\partial t^2} - k_p^2 \right) E_z = \frac{4\pi}{c} \frac{\partial \rho_b}{\partial t} + 4\pi \frac{\partial}{\partial z} (\rho_b + \rho_p) \quad (2.19)$$

using $\nabla^2 = \nabla_{\perp}^2 + \frac{\partial^2}{\partial z^2}$, in Fourier transform space, where

change this to $E=\text{integral tilde } E$, then substitute that into the following equations, since the RHS of 2.14 is not correct, fourier transform of the derivative acting on the function is not the same as the derivative acting on the transformed function

$$E_z(\xi)(k) = \int_{-\infty}^{\infty} \tilde{E}_z(k) e^{ik\xi} dk , \quad (\rho_b(k) + \rho_p(k)) = \int_{-\infty}^{\infty} (\tilde{\rho}_b(\xi) + \tilde{\rho}_p)(\xi) e^{ik\xi} d\xi \quad (2.20)$$

such that

$$\left(\frac{\partial^2}{\partial z^2} - \frac{1}{c^2} \frac{\partial^2}{\partial t^2} \right) E_z(\xi) = 0 \quad (2.21)$$

and

$$\frac{4\pi}{c} \frac{\partial \rho_b}{\partial t} + 4\pi \frac{\partial}{\partial z} (\rho_b + \rho_p) = -4\pi i k \tilde{\rho}_b + 4ik\pi \tilde{\rho}_b + 4ik\pi \tilde{\rho}_p = 4ik\pi \tilde{\rho}_p \quad (2.22)$$

which gives

$$\left(\nabla_{\perp}^2 - k_p^2 \right) \tilde{E}_z(\xi) = 4\pi i k \tilde{\rho}_p \quad (2.23)$$

We note that the two contributions from the beam cancel each other out, this is because of relativistic effects (?) [?]. From eq. XXX we have

$$\frac{\partial^2 \rho_p}{\partial t^2} + \omega_p^2 \rho_p = -\omega_p^2 \rho_b \Rightarrow -k^2 \tilde{\rho}_p + k_p^2 \tilde{\rho}_p = -k_p^2 \tilde{\rho}_b \Rightarrow \tilde{\rho}_p = \frac{k_p^2}{k^2 - k_p^2} \tilde{\rho}_b \quad (2.24)$$

$$\nabla_{\perp}^2 = \frac{1}{r} \frac{\partial}{\partial r} r \frac{\partial}{\partial r} + \frac{1}{r^2} \frac{\partial^2}{\partial \phi^2} \quad (2.25)$$

$$\left(\frac{\partial^2}{\partial r^2} + \frac{1}{r} \frac{\partial}{\partial r} - k_p^2 \right) \tilde{E}_z = 4\pi i k_p^2 \frac{k}{k^2 - k_p^2} \tilde{\rho}_b \quad (2.26)$$

We now rewrite this equation as

$$\mathcal{L} \tilde{E}_z = \tilde{f}(r) \quad (2.27)$$

We proceed as before and solve this PDE by finding the Green's function. Working in a cylindrical coordinate system we have that the Green's function must satisfy

$$\mathcal{L} G(\mathbf{r}, \mathbf{r}') = \delta(\mathbf{r} - \mathbf{r}') = \frac{1}{r} \delta(r - r') \delta(\phi - \phi') \delta(z - z') \quad (2.28)$$

where the RHS is the 3D Dirac delta function in cylindrical polar coordinates, defined such that $\int \delta(\mathbf{r} - \mathbf{r}') r dr d\phi dz = 1$. Letting

$$G(\mathbf{r}, \mathbf{r}') = G_r(r, r') \delta(\phi - \phi') \delta(z - z') \quad (2.29)$$

leads to

$$\mathcal{L} G_r(r, r') = \frac{1}{r} \delta(r - r') \quad (2.30)$$

2. Theory

The LHS of this expression is the modified Bessel function of order zero and the RHS represents our source term. Consequently the Green's function is formed by linear combinations of, the linearly independent, modified Bessels functions of order zero.

$$G(r, r') = \begin{cases} A(r')(A_1 I_0(k_p r) + B_1 K_0(k_p r)) & , 0 < r < r' \\ B(r')(A_2 I_0(k_p r) + B_2 K_0(k_p r)) & , r' < r < \infty \end{cases} \quad (2.31)$$

requiring that the two parts of this expression each satisfy one of the B.Cs we have that $B_1 = A_2 = 0$ since $K_0(k_p r) \rightarrow \infty$ as $r \rightarrow 0$ and $I_0(k_p r) \rightarrow \infty$ as $r \rightarrow \infty$. Continuity in $G(r, r')$ at $r = r'$ further gives that

$$G(r, r') = A_0 \begin{cases} I_0(k_p r)K_0(k_p r') & , 0 < r < r' \\ I_0(k_p r')K_0(k_p r) & , r' < r < \infty \end{cases} \quad (2.32)$$

where A_0 is a constant of proportionality that we find by integrating $\mathcal{L}G(r, r') = \delta(r - r')/r$ with respect to r across the interval $[r' - \epsilon, r' + \epsilon]$, which needs to be satisfied for all ϵ , including the limit as $\epsilon \rightarrow 0$.

$$\lim_{\epsilon \rightarrow 0} \int_{r'-\epsilon}^{r'+\epsilon} \left(\frac{\partial^2 G}{\partial r^2} + \frac{1}{r} \frac{\partial G}{\partial r} - k_p^2 G \right) dr = \lim_{\epsilon \rightarrow 0} \int_{r'-\epsilon}^{r'+\epsilon} \frac{1}{r} \delta(r - r') dr = \frac{1}{r'} \quad (2.33)$$

$$\lim_{\epsilon \rightarrow 0} \left[\frac{1}{k_p} \frac{\partial G}{\partial r} \right]_{z-\epsilon}^{z+\epsilon} = \frac{A_0}{k_p} \left(I_0(k_p r') \frac{\partial K_0(k_p r)}{\partial r} - \frac{\partial I_0(k_p r)}{\partial r} K_0(k_p r') \right) \Big|_{r=r'} = \frac{1}{r'} \quad (2.34)$$

This equality must hold for all values of r' . Hence, following an approach by Jackson [1], we evaluate the LHS for $r' \gg 1$, where I_0 and K_0 take the limiting forms

$$I_0(k_p r') \rightarrow \frac{1}{\sqrt{2\pi k_p r'}} e^{k_p r'} \quad \text{and} \quad K_0(k_p r') \rightarrow \sqrt{\frac{\pi}{2k_p r'}} e^{-k_p r'} \quad (2.35)$$

which implies that $A_0 = -1$. Here Gessner gets $A = 4\pi$ because of Jackson but I don't see why.

$$G(r, r') = -I_0(k_p r)K_0(k_p r')\Theta(r' - r) - I_0(k_p r')K_0(k_p r)\Theta(r - r') \quad (2.36)$$

We can thus find \tilde{E}_z from

$$\tilde{E}_z(r, k) = \int_{-\infty}^{\infty} G(r, r') f(r', k) r' dr' \quad (2.37)$$

and then perform an inverse Fourier transform to find

$$E_z(r, \xi) = \frac{1}{2\pi} \int_{-\infty}^{\infty} \tilde{E}_z(r, k) e^{ik\xi} dk \quad (2.38)$$

Doing this yields

$$E_z(r, \xi) = \frac{4\pi i k_p^2}{2\pi} \int_{-\infty}^{\infty} \frac{ke^{ik\xi}}{k^2 - k_p^2} dk \int_0^{\infty} G(r, r') \tilde{\rho}_b(r') r' dr' \quad (2.39)$$

$$= -2\pi k_p^2 \cos(k_p \xi) \Theta(\xi) \int_0^{\infty} G(r, r') \tilde{\rho}_b(r') r' dr' \quad (2.40)$$

Where the $\Theta(\xi)$ has been added due to causality.

Now lets solve this for a bi-Gaussian beam charge distribution. To do this, we may compute the electric field from the Green's function directly and then carrying out the inverse Fourier transform, or we could choose to first compute the field due to a point-particle and then convolving it with the bi-Gaussian distribution. We proceed by doing the latter by choosing a charge distribution with radial symmetry and a delta function in the z -direction to match our Green's function.

$$\rho_{b_0}(r, \xi) = \frac{e}{2\pi r} \delta(r - r_0) \delta(\xi) \Rightarrow \tilde{\rho}_{b_0}(r, k) = \int_{-\infty}^{\infty} \rho_b(r, \xi) e^{-ik\xi} d\xi = \frac{e}{2\pi r} \delta(r - r_0) \quad (2.41)$$

which gives

$$\tilde{E}_z(r, k) = -2ek_p^2 \frac{k}{k^2 - k_p^2} G(r, r_0) \quad (2.42)$$

which satisfies (2.26), as can be shown by integrating across the discontinuity and taking the limit to zero, and then gives

$$E_z(r, \xi) = -ek_p^2 \cos(k_p \xi) G(r, r_0) \Theta(\xi) \quad (2.43)$$

But my Green's function has a $A = -1$ as constant and not $A = 4\pi$ as Bonatto and Gessner
 This is refer to as the single-particle wake function [?]. The longitudinal electric field resulting from an arbitrary source distribution $n_b(r, \xi)$ is given by the convolution of the source by the single-particle wake function:

$$E_z(r, \xi) = -ek_p^2 \int_{-\infty}^{\infty} \cos(k_p(\xi - \xi')) \Theta(\xi - \xi') d\xi' \int_0^{\infty} G(r, r_0) n_b(r_0, \xi') r' dr' \quad (2.44)$$

$$= -ek_p^2 \int_{-\infty}^{\xi} \cos(k_p(\xi - \xi')) d\xi' \int_0^{\infty} G(r, r_0) n_b(r_0, \xi') r_0 dr_0 \quad (2.45)$$

which is not the same as Bonatto/Gessner/Schroeder, the limits are different, they have from xi to infinity , is this not how to do a convolution? Why don't we have something like $r - r'$ from a radial convolution or something? Bonatto, Schroder has the integral from infinity to xi, why?

These expressions with -4π does not satisfy the diff.eq that I am trying to solve in transform space, so why do they use them if they don't solve their original diff. equations?

Mira's thesis also has 4π if converting to cgs.

2.1.4 Transverse Focusing Field

Use Panofsky-Wenzel theorem

2.2 Non-linear Regime

2.2.1 Wave-breaking field

Dawson's derivation [Note: The wave-breaking field does not represent the onset of the non-linear regime but the highest achievable field in the non-linear regime.] We consider a simple 1D linear non-relativistic electron sheet model first used by Dawson [2] to show the breakdown of the linear model (**correct?**). Consider the plasma being made up of thin sheets of ions and electrons. A sheet at equilibrium position $z = z_0$ is then displaced by $\eta_0(z_0)$, where the displacement is set as function of the equilibrium position for full generality, to a new position $z = z_0 + \eta_0$. The displaced sheet reveals a positive surface charge density $\sigma = en_0\eta_0$, where n_0 is the electron charge density in the plasma. This sets up a restoring electric field which we find using Gauss's law to be $E_{\text{res}} = 4\pi n_0 e \eta_0$ which yields a restoring force

$$m_e \frac{\partial^2 \eta_0}{\partial t^2} = -eE_{\text{res}} = -4\pi n_0 e^2 \eta_0 = -\omega_p^2 \eta_0 \quad (2.46)$$

with solutions

$$\eta_0(z_0, t) = A_1(z_0) \cos(\omega_p t) + A_2(z_0) \sin(\omega_p t) \quad (2.47)$$

The phenomena of wave breaking can be shown by considering another electron sheet at an equilibrium position $z_1 = z_0 + \Delta z_0$ at a distance Δz_0 away from the first sheet. This sheet is then displaced by η_1 to a new position $z_1^* = z_0 + \Delta z_0 + \eta_1$. The linear model is valid provided that there are no electron trajectories intersect one another in the plasma [**is this correct? Why does the model break down?**]. Hence the model is valid provided that $z_1^* - z_0 > z - z_0$ which implies that we must have

$$\Delta z_0 + \eta_1 > \eta_0 , \quad (2.48)$$

for all $\Delta z_0 \in \mathbb{R}$, to sustain plasma oscillations in the linear model. We now consider the limit as $\Delta z_0 \rightarrow 0$ for the expression

$$\frac{\partial \eta}{\partial x_0} = \lim_{\Delta z_0 \rightarrow 0} \frac{\Delta \eta}{\Delta z_0} = \lim_{\Delta z_0 \rightarrow 0} \left(\frac{\eta_1 - \eta_0}{\Delta z_0} \right) > \lim_{\Delta z_0 \rightarrow 0} \left(\frac{\eta_0 - \Delta z_0 - \eta_0}{\Delta z_0} \right) = -1 \quad (2.49)$$

which simplifies to

$$\frac{\partial \eta}{\partial z_0} > -1 \quad (2.50)$$

where the inequality is introduced using Eq. (2.48). We now consider the special case where $A_1(z_0) = A \sin(k_p z_0)$ and $A_2(z_0) = 0$. This is a valid solution since $\sin(k_p z_0)$ is single-valued for all $k_p, x_0 \in \mathbb{R}$. This particular solution is chosen to highlight the breakdown of the electric field, and is motivated by ([what?]) the solution we found for the electric field in section 2. Applying the no-crossing criterion in Eq. 2.50 to $\eta = \eta_0(z_0, t)$ yields

$$\frac{\partial \eta_0}{\partial z_0} = Ak_p \cos(k_p z_0) > -1 \Leftrightarrow Ak_p \leq 1 \quad (2.51)$$

which gives the maximum amplitude as $A_{\max} = 1/k_p$. Hence the maximum restoring electric field $E_{\max} \equiv E_{\text{wb}} = 4\pi n_0 / k_p$ is given by

$$E_{\text{wb}} = \frac{m_e v_p \omega_p}{e} \quad (2.52)$$

the so-called *wave-breaking field*. To further show how this breaks the linear model we consider the effect on the electric field up to and past the wave-breaking limit. As above we have,

$$z = z_0 + \eta_0 = z_0 + A \sin(k_p z_0) \quad (2.53)$$

and

$$E = 4\pi n_0 e A \sin(k_p z_0) \quad (2.54)$$

from which we want to find the electric field as a function of z . We can do this by numerically solving Eq. 2.53 for z_0 in a range of z values given fixed values of A . This gives $z_0 = z_0(z, A)$ which can be substituted into Eq. 2.54 to give $E = E(z, A)$, the result of which is shown in Fig. 2.1. From this we conclude that the electric field is no longer single-valued for $A > 1/k_p$, i.e past the electric field's wave-breaking amplitude, which signifies a breakdown of the linear model.

This is further emphasized by consider the electron-density response as $\partial\eta/\partial z_0 \rightarrow -1$. To do this we use Eq. XXX in 1D with no beam density $n_b = 0$,

$$\frac{\partial E}{\partial z} = 4\pi e(n_0 - n) \quad (2.55)$$

where $n = n_0 + n_1$ is the perturbed plasma density and n_0 is the ion density, hence $n_0 - n$ is the free (negative) charge density in the plasma. We now take the derivative of the perturbed electric field and substitute the above expression

$$\frac{\partial E}{\partial z} = 4\pi n_0 e \frac{\partial \eta}{\partial z} \Rightarrow n = n_0 \left(1 - \frac{\partial \eta}{\partial z}\right) \quad (2.56)$$

We now rewrite $\partial/\partial z$, using $z = z_0 + \eta$, as

$$\frac{\partial}{\partial z} = \left(1 - \frac{\partial \eta}{\partial z_0}\right)^{-1} \frac{\partial}{\partial z_0} \quad (2.57)$$

which gives

$$n = \frac{n_0}{1 + \frac{\partial \eta}{\partial z_0}} \quad (2.58)$$

which means that the perturbed electron density grows infinite as $\partial\eta/\partial z_0 \rightarrow -1$, again signifying the breakdown of the linear model.

Having seen that the linear theory can break down mathematically, it is crucial to ask whether this is realised in 3D models and experiments as well.

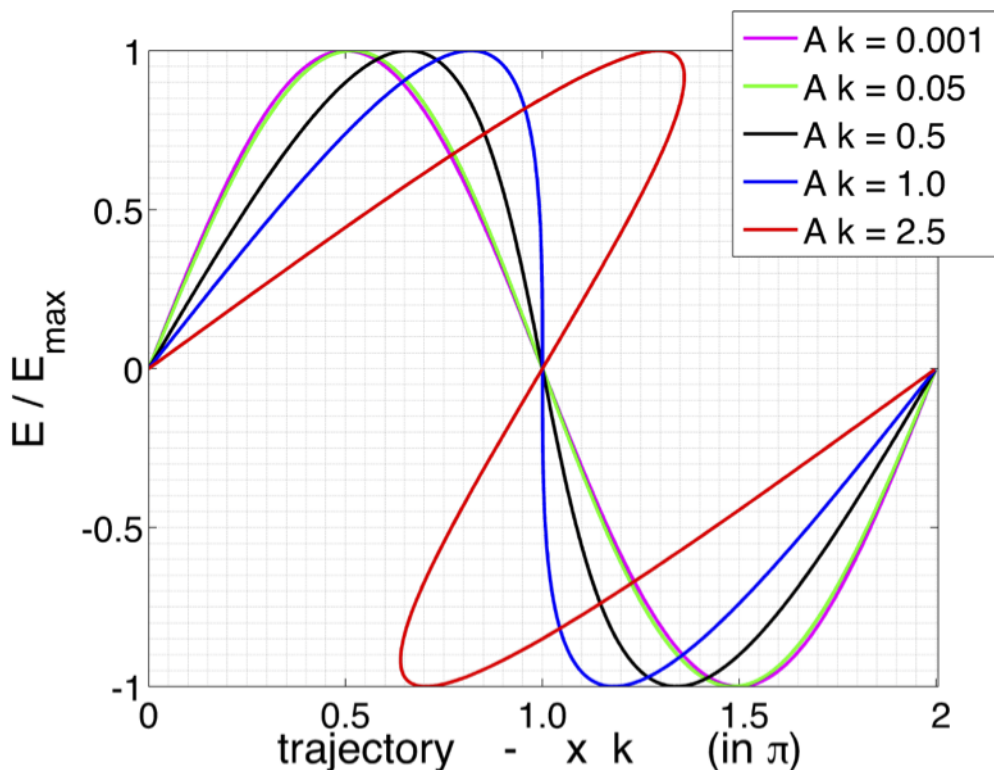


Figure 2.1: Plot corresponding to Dawson's derivation of the wave-breaking field [ref. Sahai].

2.3 Particle interactions with matter

Conventional beam dumps work by stochastic interactions of the beam with the dense medium [hanahoe 6.5]

2.3.1 Bohr-Fermi-Bethe-Bloch Theory

Bethe-Bloch formula:

$$-\left\langle \frac{dU}{ds} \right\rangle_{ion} = \frac{4\pi e^4 n_{e,m}}{m_e c^2 \beta^2} \left[\ln \left(\frac{2m_e \gamma^2 v^2}{I} \right) - \beta^2 \right] \quad (2.59)$$

2.3.2 Collective Plasma Deceleration – Non-Linear regime

$$-\left(\frac{dE}{dz} \right)_{coll-wave-break} = F_e = eE_{wave-break} = m_e c \omega_p \left(\frac{n_b}{n_e} \right) \quad (2.60)$$

What is the wave-breaking electric field?

2.3.3 Collective Plasma Deceleration – Linear regime

Based on the work of Lu et. al [3], wherein it was shown that the predictions from the linear models perform well even in the non-linear regime, it is of interest to compute the energy loss in the linear regime. This follows the analysis by Bonatto et al. [4].

The energy loss of a bunch is due to the work carried out by the longitudinal electric field E_z , neglecting effects such as bremsstrahlung etc. The rate of energy change with propagation distance of a particle at position (r, ξ) in the bunch after travelling is given by the force exerted on the particle by the longitudinal electric field:

$$\frac{dU_p}{ds} = -eE_z(r, \xi) \quad (2.61)$$

where we have assumed that there occurs no modulation of the particle bunch as it traverses the plasma, hence the electric field is only a function of the position in the bunch $E_z(r, \xi)$ and not the propagation distance s . Integrating over the propagation distance then gives the energy of one particle in the beam at position (r, ξ) after travelling a distance s :

$$U_e(r, \xi, s) = U_e(r, \xi, 0) - seE_z(r, \xi) \quad (2.62)$$

from which multiplication by the beam number density $n_b(r, \xi)$ and integration over the volume of the bunch gives the total energy of all particles in the bunch after propagation distance s

$$U(s) = \int U_e(r, \xi, 0) n_b(r, \xi) r dr d\xi d\phi - se \int E_z(r, \xi) n_b(r, \xi) r dr d\xi d\phi \quad (2.63)$$

where $dV = r dr d\xi d\phi$ [I think].

2.3.4 Notes Bonatto

Rate of change due to the longitudinal electric field acting on an electron beam, i.e position beam in the decelerating region of the wakefield.

"the beam only experiences its self-excited wakefield."

In the passive beam dump, are we essentially slowing down a "drive bunch" without having a witness bunch behind to get accelerated?

It is probably better to use gamma as in Bonatto's paper, to make it easier to explain total beam energy integral. Basically integrate over all particles.

$$U = \gamma m_e c^2$$

$$-\frac{dU}{ds} = (F_e)_z = eE_z \quad (2.64)$$

where s is the distance travelled in the plasma and U is the energy of a particle in the beam at position ξ . for ultra relativistic beams, $\beta \sim 1$, the longitudinal electric field is a function of the position along the bunch $\xi = z - ct$ and not z explicitly.

$$U(s, \xi) = U_0 - esE_z(\xi) \quad (2.65)$$

The total energy of the beam after travelling a distance s is then found by integrating across all the particles in the beam, which is integrating across ξ since analysis is in 1-D.

$$\mathcal{U}(s) = U_0 \int_{-\infty}^{\xi} \dots \quad (2.66)$$

We will proceed by calculating the gamma factor of a given particle in the beam who's energy we wish to compute.

$$\gamma(s, \xi) = \gamma_0 - esE_z(\xi) \quad (2.67)$$

3

Simulations

- Ways to simulate plasmas, different techniques/codes etc.

3.1 Particle-in-Cell Simulations

Why simulations

The highly non-linear features present in the high-energy plasma wakefield phenomena we wish to model do not lend themselves easily to analytical treatments. Fortunately, simulations allow us to study, understand and exploit these phenomena without the need to repeatedly perform expensive and intricate experiments.

Why use PIC? How Pic works.

The response of the plasma to the propagation of an electron beam could theoretically be simulated by, at time t_0 , solving Maxwell's equations and calculating the combined electromagnetic fields acting on each particle in the plasma and beam, then by considering each particles velocity could calculate the new positions and velocities of all particles for a small time increase $t_0 + \Delta t$. Repeating these computation would in theory lead us to find the approximate plasma response at any arbitrary time t . This approach is however computationally impossible if we attempt this approach is however computationally unattainable in most plasma simulations. For instance, if we consider that the plasma in a typical plasma wakefield accelerator [Hanahoe] is on the order of centimetres in extent, with a number density $10^{20} m^{-3}$, we find that we have on the order of 10^{14} electrons in the plasma. All these electrons would have to be included in the simulation and stored with their associated 6-dimensional position and velocity data (x, y, z, v_x, v_y, v_z) . Each number would be stored as a 32-bit double precision floating point number, yielding the total data size required for the whole plasma simulation on the order of a petabyte (10^{15} bytes).

To circumvent this computational road block we make use of Particle-In-Cell (PIC) codes. The key feature of PIC codes is to represent large collections of physical microscopic particles as smaller collections of macroscopic pseudo-particles, where each macroscopic particle carries the total charge and mass of the microscopic particles it represents. The behaviour of these macro particles is then calculated and used as a representation of the response of the actual plasma.

3.1.1 EPOCH

Is a second order (?) relativistic P.I.C. code

1D,2D or 3D options.

The simulations presented in this thesis are generated using the open-source plasma physics

3. Simulations

PIC simulation code EPOCH, which is based upon the particle push and field update algorithms of the SRC code [ref]. [compare with fig3.1 hanahoe thesis]

Starting from EM fields $\mathbf{E}_{(n)}$, $\mathbf{B}_{(n)}$ and charge current $\mathbf{J}_{(n)}$ present at iteration n [at a specific position, middle of Yee grid?] we obtained the fields at the next time step $n+1$ by computing the resulting fields and currents at an intermediate half-way step $n+1/2$. We do this by first computing the change in the electric field, using Ampere's law, $\Delta\mathbf{E}_{(n)}$ which we add to our current field such that

$$\mathbf{E}_{(n+1/2)} = \mathbf{E}_{(n)} + \frac{\Delta t}{2} \left(c^2 \nabla \times \mathbf{B}_{(n)} - \frac{\mathbf{J}_{(n)}}{\epsilon_0} \right) \quad (3.1)$$

from this the magnetic field is given by

$$\mathbf{B}_{(n+1/2)} = \mathbf{B}_{(n)} - \frac{\Delta t}{2} \left(c^2 \nabla \times \mathbf{E}_{(n+1/2)} \right) \quad (3.2)$$

(at which point the particle pusher, detailed below, updates the current to $\mathbf{J}_{(n+1)}$)
at which point we need to update the current to $\mathbf{J}_{(n+1)}$ in order to proceed finding the fields at time step $n+1$. This is done using the particle pusher. We update the position of each particle

$$\mathbf{x}_{(n+1/2)} = \mathbf{x}_{(n)} + \frac{\Delta t}{2} \mathbf{v}_{(n)} \quad (3.3)$$

from which we also obtain the intermediate velocity $\mathbf{v}_{(n)}$ [correct?]. Using the Lorentz force law we then compute the force $\mathbf{F}_{(n)} = \Delta p / \Delta t$ which gives the momentum at $n+1$ as

$$\mathbf{p}_{(n+1)} = \mathbf{p}_{(n)} + q \Delta t \left[\mathbf{E}_{(n+1/2)} \left(\mathbf{x}_{(n+1/2)} \right) + \mathbf{x}_{(n+1/2)} \times \mathbf{B}_{(n+1/2)} \left(\mathbf{x}_{(n+1/2)} \right) \right] \quad (3.4)$$

where, the electric fields are extrapolated (?) to the intermediate point $n+1/2$. Then, using $\mathbf{p} = \gamma m \mathbf{v}$, we can find the velocity at $n+1$, from which we then have the current $\mathbf{J}_{(n+1)}$. We then reverse the order of computing such that the magnetic field is calculated prior to the electric field,

$$\mathbf{B}_{(n+1)} = \mathbf{B}_{(n+1/2)} - \frac{\Delta t}{2} \left(c^2 \nabla \times \mathbf{E}_{(n+1/2)} \right) \quad (3.5)$$

$$\mathbf{E}_{(n+1)} = \mathbf{E}_{(n+1/2)} + \frac{\Delta t}{2} \left(c^2 \nabla \times \mathbf{B}_{(n+1)} - \frac{\mathbf{J}_{(n+1)}}{\epsilon_0} \right) \quad (3.6)$$

Using these fields when then calculate the new particles positions $\mathbf{x}_{(n)}$, we "push" the particles, thus completing the iteration step.

3.1.2 Grid settings

An important feature of PIC codes is the grid parameters. When setting up the resolution of the grid one has to make sure that the grid is sufficiently fine such that the smallest features of our physical system are resolved. This is to ensure that the simulation accurately models the physical system it is meant to represent, to the extent that missing small scale phenomena might alter the large scale outcome of the simulation. A finer grid however requires more macroparticles to fully populate the grid, which inevitably extends the computational time. In addition the time step Δt needs to be suitably decreased as well. This

is because of the so-called Courant-Friedrichs-Lowy (CFL) condition. Any simulation introduces uncertainties in the final outcome due to the finite resolution. We need to make sure that the uncertainties introduced during each iteration do not build up and grow unbounded.

Parameters and initial conditions are defined using an *input.deck* file.

```
begin:boundaries
  bc_x_min = simple_laser
  bc_x_max = simple_outflow
  bc_y_min = simple_outflow
  bc_y_max = simple_outflow
end:boundaries

$$n_b = \frac{1}{\sigma_x \sigma_y^2 (2\pi)^{3/2}} e^{-(x-x_0)^2/2\sigma_x^2} e^{-(y-y_0)^2/2\sigma_y^2} e^{-(z-z_0)^2/2\sigma_z^2}$$

```

3.2 Notes.

Meeting Guoxing:

- We will change $\sigma_{x,y}$, in simulation from $\sigma_{x,y} = 0.3\mu m \rightarrow 5 - 10\mu m$ because the $0.3\mu m$ EuPRAXIA beam parameter gives to high beam density n_b , which means that we can't have $n_b \sim n_p$ because the plasma density would have to be too high. We should aim for $n_p \sim 10^{17} - 10^{18} \sim n_b$ (standard L/PWFA) parameters. EuPRAXIA wants $\sigma_{x,y}$ small because small bunches gives more coherent radiation in undulators. One could expand the beam by letting it propagate freely (expand due to space charge) a distance before reaching the beam dump.

- Run simulations with uniform plasma density for
$$\begin{cases} n_p \sim 0.1n_b & \text{Non-linear} \\ n_p \sim n_b & \text{Quasi-linear} \\ n_p \sim 10n_b & \text{Linear} \end{cases}$$
- Use $\Delta E/E = 0.01$ and bunch charge 30 pC (5 fs).
- Estimate necessary simulation propagation length by saturation length using wave-breaking electric field gradient

$$L_{\text{sat}} \approx \frac{T_0}{eE_{\text{wb}}} = \frac{T_0}{e} \frac{e}{m_e c \omega_p} = \frac{T_0}{m_e c} \sqrt{\frac{m_e e \epsilon_0}{e^2 n_b}}$$

- Project outline:
 - Uniform plasma with varying $n_b \sim n_p$
 - Vary plasma density profile
 - Test laser to dump head of beam
 - Run simulations for real FlashForward parameters and not the idealized EuPRAXIA parameters.
- 100pC

$$n_b = \frac{N_p}{(2\pi)^{3/2} \sigma_y^2 \sigma_x} = \frac{6.25 \times 10^8}{(2\pi)^{3/2} (5 \times 10^{-6})^3} \approx 3.2 \times 10^{23} \text{ m}^{-3}$$

$$\Rightarrow eE_{\text{wb}} = \begin{cases} 17 \text{ GeV/m} & n_p = 0.1n_b \\ 54 \text{ GeV/m} & n_p = n_b \\ 172 \text{ GeV/m} & n_p = 10n_b \end{cases} \Rightarrow L_{\text{sat}}(1 \text{ GeV}) = \begin{cases} 5.8 \text{ cm} & n_p = 0.1n_b \\ 1.9 \text{ cm} & n_p = n_b \\ 0.6 \text{ cm} & n_p = 10n_b \end{cases}$$

$$1 \text{ GeV beam} \Rightarrow L_{\text{sat}} \sim 2 \text{ cm} = 2 * 10^4 \mu\text{m}$$

- 30pC

$$n_b = \frac{N_p}{(2\pi)^{3/2} \sigma_y^2 \sigma_x} = \frac{1.87 \times 10^8}{(2\pi)^{3/2} (5 \times 10^{-6})^3} \approx 9.5 \times 10^{22} \text{ m}^{-3}$$

$$\Rightarrow eE_{\text{wb}} = \begin{cases} 9.4 \text{ GeV/m} & n_p = 0.1n_b \\ 30 \text{ GeV/m} & n_p = n_b \\ 94 \text{ GeV/m} & n_p = 10n_b \end{cases} \Rightarrow L_{\text{sat}}(1 \text{ GeV}) = \begin{cases} 10.7 \text{ cm} & n_p = 0.1n_b \\ 3.4 \text{ cm} & n_p = n_b \\ 1.1 \text{ cm} & n_p = 10n_b \end{cases}$$

$$1 \text{ GeV beam} \Rightarrow L_{\text{sat}} \sim 3.4 \text{ cm} = 3.4 * 10^4 \mu\text{m}$$

4

Preliminary Results

4.1 Plasma deceleration - Uniform and varying density

4.2 Hybrid Scheme - Feasibility study

4.2.1 Initialising a decelerated bunch

-Compare to actual already propagated bunch we want to simulate. See how quickly the uniform plasma resembles that of the plasma of the propagated simulation. If it takes long time then the laser results might not represent the real situation. Compare simulations side by side as both real and initialised bunches propagate further, see if any deviations occur or if the bunch I set up is actually a fair approximation (compare energy, particle number etc.)

4.2.2 Introduction of co-propagating laser

- Results with respect to laser intensity/amplitude/wavelength as well as distance from bunch.

4. Preliminary Results

5

Conclusion

Lorem ipsum dolor sit amet, consectetur adipisicing elit, sed do eiusmod tempor incididunt ut labore et dolore magna aliqua. Ut enim ad minim veniam, quis nostrud exercitation ullamco laboris nisi ut aliquip ex ea commodo consequat. Duis aute irure dolor in reprehenderit in voluptate velit esse cillum dolore eu fugiat nulla pariatur. Excepteur sint occaecat cupidatat non proident, sunt in culpa qui officia deserunt mollit anim id est laborum.

5. Conclusion

Bibliography

- [1] John David Jackson. Jackson - Classical Electrodynamics (3rd Ed.).pdf, 1962.
- [2] John M Dawson. Electron Oscillations in a Cold Plasma. Technical Report 2, 1959.
- [3] W. Lu, C. Huang, M. Zhou, M. Tzoufras, F. S. Tsung, W. B. Mori, and T. Katsouleas. A nonlinear theory for multidimensional relativistic plasma wave wakefields. *Physics of Plasmas*, 13(5), 2006.
- [4] A. Bonatto, C. B. Schroeder, J. L. Vay, C. R. Geddes, C. Benedetti, E. Esarey, and W. P. Leemans. Compact disposal of high-energy electron beams using passive or laser-driven plasma decelerating stage. *AIP Conference Proceedings*, 1777(1):0–5, 2016.

Bibliography

A

Appendix: Input decks